Brazilian Journal of Physics (2026) 56:38
https://doi.org/10.1007/s13538-025-01963-y

# Chemoimmunotherapy in Non-small Cell Lung Cancer Control

**Ana P. S. Koltun[1] · Moises S. Santos[3] · José Trobia[2] · Fernando S. Borges[1,4] · Kelly C. Iarosz[1,5] · Iberê L. Caldas[6] · Enrique C. Gabrick[6] · Diogo L. M. Souza[1] · Fátima E. Cruziniani[1] · Antonio M. Batista[1,2]**

Received: 7 October 2025 / Accepted: 19 November 2025 / Published online: 10 December 2025


**Abstract**
The term cancer is generally used to refer to a large group of diseases. Neoplastic or cancerous cells grow and divide in an uncontrolled manner and, as a result, form tumours that progressively increase in size. There are different types of cancer which are categorised according to the type of tissue or fluid originated from inside the body. We incorporate chemotherapeutic agents into a mathematical model of non-small cell lung cancer interacting with immune cells. The immune system cells included in the model are composed of macrophages and cytotoxic lymphocytes. In our model, tumour infiltrating lymphocyte therapy is also considered. In this work, we show how pulsed chemotherapy combined with immunotherapy, known as chemoimmunotherapy, can improve survival outcomes in the treatment of non-small cell lung cancer.

**Keywords** Macrophage · Cancer model · Non-small cell lung cancer · Chemotherapy treatment · Immunotherapy

## 1 Introduction

Cancer is a group of diseases characterised by the uncontrolled growth of abnormal cells. Healthy cells can be recruited and transformed into pathological cells. There are over 100 types of cancer, including skin, breast, leukemia, and lung cancer [1]. In the United States, it was estimated that there would be approximately 2 million cases of invasive cancer and around 600,000 cancer-related deaths in 2024 [2]. Among the vast number of cancer types, lung cancer is the second leading cause of cancer related death. It is primarily classified into non-small cell lung cancer (NSCLC) and small cell lung cancer (SCLC) [3]. NSCLC is known to be the most lethal cancer type worldwide [4]. Due to diversity of cells in its microenvironment, multiple clinical treatments have been explored and developed [5, 6].

In the past few decades, several cancer treatments have been proposed, such as radiotherapy, chemotherapy, and immunotherapy [7]. Chemotherapy is one of the most common treatments for various types of cancers [8]. This treatment consists of eliminating fast-proliferating cells, such as cancer cells. However, this approach also damages healthy fast-growing cells [8–11]. The time interval between chemotherapy sessions is crucial for the treatment, allowing the healthy cells to regenerate from the damage [8]. Chemotherapy follows specific protocols regarding timing and dosage [8, 12]. In NSCLC, different chemotherapy protocols, known as ANITA, have been used. For instance, the $1\times7$ chemotherapy protocol [13–15] in which the chemotherapeutic agents are administered every seven days during a period, while $1\times21$ [15, 16] involves dosing every twenty-one days. We also

Ana P.S. Koltun, Moises S. Santos, José Trobia, Fernando S. Borges, Kelly C. Iarosz, Iberê L. Caldas, Enrique C. Gabrick, Diogo L. M. Souza, Fátima E. Cruziniani and Antonio M. Batista contributed equally to this work.

✉ Ana P. S. Koltun
anapkoltun@gmail.com

[1] Graduate Program in Science, State University of Ponta Grossa, 84030-900 Ponta Grossa, PR, Brazil

[2] Department of Mathematics and Statistics, State University of Ponta Grossa, 84030-900 Ponta Grossa, PR, Brazil

[3] Municipal Secretary of Education of Ponta Grossa, Ponta Grossa, PR, Brazil

[4] Department of Physiology and Pharmacology, State University of New York Downstate Health Sciences University, Brooklyn, NY, USA

[5] University Center UNIFATEB, 84266-010 Telêmaco Borba, PR, Brazil

[6] Physics Institute, University of São Paulo, 05508-090 São Paulo, SP, Brazil

consider two cycles of combination chemotherapy, given by 1×7 plus 1×28. The use these two cycles is based on the work published by Douillard et al. [13]. They compared the effect of adjuvant vinorelbine plus cisplatin on survival in patients with NSCLC. Further details on NSCLC chemotherapy protocols can be found in References [15, 17–21].

The chemotherapy damages the healthy fast proliferating cells and, as a consequence, the immune system becomes weaker [7]. Due to this fact, some cancer treatments have shown that chemotherapy with immunotherapy can strengthen the immune system [21]. A common immunotherapy for NSCLC is the tumour-infiltrating lymphocytes (TIL) therapy [5, 21]. TIL enhances the elimination of tumour cells by injecting a large number of T cells into the body, that are predators of cancer cells [5, 22, 23].

Various mathematical models have been proposed for describing the cancer cell growth dynamics [7, 12, 24–29]. Das et al. [30] investigated a dynamic model depicting cancer growth, incorporating chemotherapy and immune system. Iarosz et al. [27] introduced a model of brain tumour where glial cells, glioma, neurons, and chemotherapeutic agents interact with one another. This model was extended to include drug resistance under continuous and pulsed chemotherapy [25]. In the extended model, the neuron's lifespan depends on the infusion rate of the chemotherapy and the mutation rate from drug-sensitive to drug-resistance cells. Trobia et al. [26] mathematically described the interaction among the immune system, cancer cells, and anti-cancer drugs. Their findings suggest that the delay in the immune system targeting the tumour cells influences the treatment efficacy.

Cancer cell proliferation has been modelled throughout the years [28, 29], for instance the interaction among macrophage cells, immunotherapy, and NSCLC [5, 31]. The macrophage cells M1 and M2 are white blood cells responsible for eliminating pathogens. They can not only stop the spread of cancer cells, but also promote the cancer growth. Eftimie et al. [31] proposed a model capable of reproducing the dynamics of NSCLC considering the M1 and M2 macrophages. They showed that the macrophage half-lives affect the treatment outcome. Lourenço et al. [5] studied the interaction among NSCLC, macrophages (M1 and M2), and CD8+ T cells when TIL immunotherapy is applied. They demonstrated that the growth and death rate of M1 as well as CD8+ T cells growth rate can affect the reduction of NSCLC.

In this work, we modify the NSCLC model published by Lourenço et al. [5]. The model consists of four differential equations, each one representing a different type of cell, given by NSCLC, M1, M2, and CD8+ T cells. The TIL therapy is also considered in our model. We include chemotherapy to investigate how different treatment protocols influence the reduction of the NSCLC. Our results show how the combination of TIL with different chemotherapy protocols can effectively increase the number of days that the tumour takes to regrow, improving the post-treatment status.

The paper is organised as follows: In Section 2, we discuss the mathematical model. In Section 3, we present our results regarding the different chemotherapy protocols and immunotherapy. In Section 4, we draw our conclusions.

## 2 Mathematical Model

We include chemotherapy in a cancer model [5, 9, 33] incorporating a constant source of macrophages in the tumour microenvironment. Depending on the phenotypic signaling, the macrophages can be activated. The model also considers tumour-infiltrating lymphocytes (TIL), which consists of removing T lymphocyte cells and injecting back into the tumour microenvironment [5, 32]. Figure 1 displays a schematic representation of the interactions included in our modified model. The number of tumour neoplastic cells is denoted by $N$, the numbers of macrophage phenotype 1 and 2 cells are represented by $M_1$ and $M_2$, respectively, and $T_8$ is related to the number of immune system cells (CD8+ T cells). The arrows indicate the interactions and biological processes involving these cells.

Considering chemotherapy in the NSCLC model, our model is given by

$$\frac{dN}{dt} = \alpha_1 N\left(1-\frac{N}{K_n}\right)(1+\alpha_2 M_2) - \beta_1 M_1 N - N\left(\beta_2 T_8 + \frac{a_1 Q}{b_1+N}\right), \tag{1}$$

$$\frac{dM_1}{dt} = \lambda m_0 + \alpha_3 M_1\left(1-\frac{M_1+M_2}{K_m}\right) + \rho_2 M_2 - M_1\left(\rho_1 N + \mu_1 + \frac{a_2 Q}{b_2+M_1}\right), \tag{2}$$

$$\frac{dM_2}{dt} = \lambda m_0 + \alpha_4 M_2 N\left(1-\frac{M_1+M_2}{K_m}\right) + \rho_1 M_1 N - M_2\left(\rho_2 + \mu_2 + \frac{a_3 Q}{b_3+M_2}\right), \tag{3}$$

$$\frac{dT_8}{dt} = v(t) + \alpha_5 M_1 T_8\left(1-\frac{T_8}{K_t}\right) - \beta_3 M_2 T_8 - T_8\left(\mu_3 + \frac{a_4 Q}{b_4+T_8}\right), \tag{4}$$

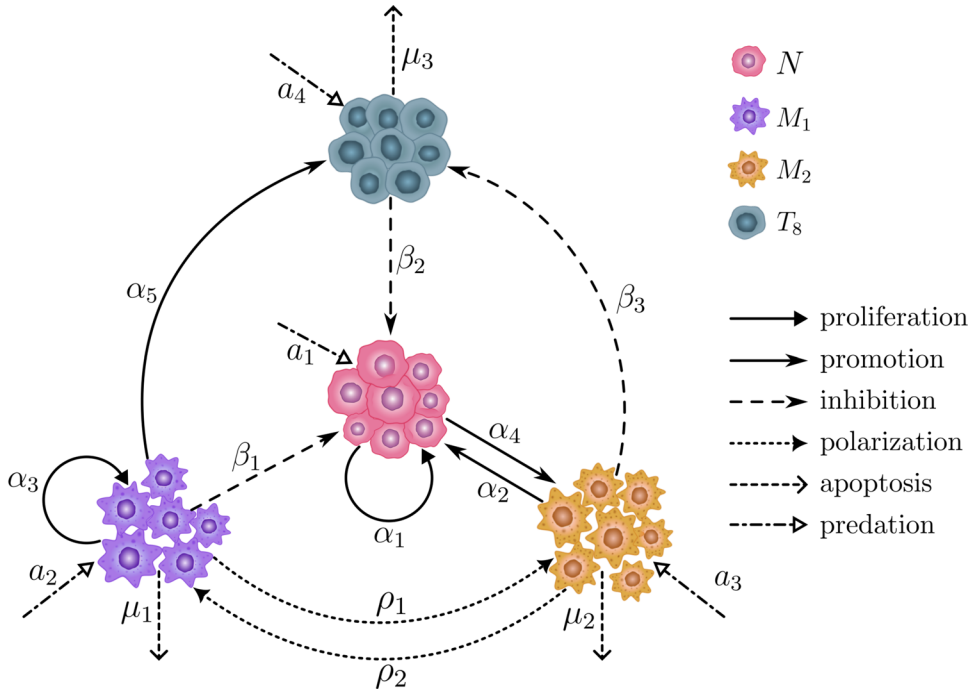


**Fig. 1** Schematic representation of our modified model, where $N$ corresponds to the number of tumour neoplastic cells, $M_1$ is the number of macrophage phenotype 1 cells, $M_2$ is the number of macrophage phenotype 2 cells, and $T_8$ is related to the number of immune system cells (CD8+ T cells). The arrows correspond to the cell interactions and biological processes

$$\frac{dQ}{dt} = \Phi - \theta Q, \tag{5}$$

where

$$v(t) = \begin{cases} 0.2857 & , t \in [7, 8] \\ 0 & , t \in (-\infty, 7) \cup (8, \infty). \end{cases} \tag{6}$$

The function $v(t)$ is related to the infusion protocol for the tumour-infiltrating lymphocyte therapy. The dose is applied continuously between the 7th and 8th days. The infusion enhances the elimination of tumours mediated by $T_8$ cells. It is a standard treatment protocol [9]. In the immunotherapy protocol, the dosage is applied only during a specified period of time. Outside this period, there is no dosage. The cell populations ($N$, $M_1$, $M_2$, and $T_8$) are limited by the carrying capacities ($K_n$, $K_m$, and $K_t$) that are equal to 1 mm$^{-3}$ [31]. The description and values of the parameters are shown in Table 1 [5].

In (1), the first term represents the growth of neoplastic cells that are influenced by the amount of $M_2$ macrophages and tumour growth factors. The second and third terms describe the reduction of $N$ due to the action of $M_1$ macrophages and CD8+ T effectors, respectively. The last term is related to the chemotherapeutic agent. In (2), the first term represents a constant source of macrophages. The second term indicates that $M_1$ depends on the number of $M_2$. The third and fourth terms represent the internal processes and chemotherapy. In the third term in (2), the macrophage repolarisation occurs in response to the signals from the microenvironment. The immune cells can change their functional phenotype, for instance from a pro-inflammatory ($M_1$) to an anti-inflammatory ($M_2$) phenotype. The parameter $\rho_2$ can be related to a background biological process and its study can play an important role in future cancer immunotherapy. The first and second terms in (3) represent the source of macrophages and the growth of $M_2$. The third and fourth terms are associated with the internal processes and chemotherapy. In (4), the second term models the number of CD8+ T effectors that are responsible for the reduction of the $N$ neoplastic cells. The third term indicates the reduction effect due to the macrophages with phenotype 2. The last equation describes the dynamics of the chemotherapeutic agent, the chemotherapy, where the first term is related to the amount of chemotherapy and the second term represents the rate of absorption of the drug in the organism. $Q$ is the chemotherapeutic agent concentration and $\theta$ is the absorption rate.

The fourth term in (2) and (3) as well as the third term in (4) correspond to the natural cell death (apoptosis). In (1), (2), (3), and (4), the last term represents a Holling type 2 interaction function, which indicates the action of the chemotherapy on the cells. The parameters are associated with the regulatory interactions that $N$, $M_1$, $M_2$, and $T_8$ have with each other, through enzymes and other biochemical mechanisms. From a mathematical point of view, we consider that the parameter values are not negative. According to the hypotheses assumed for lung cancer, positive parameter values guarantee the existence and positivity of the analytical solutions.

In Fig. 2, we compute the population dynamics of $N$ (red line), $M_1$ (black line), $M_2$ (cyan line), and

**Table 1** Parameter descriptions and values used in our simulations [5]

| Parameter | Values | Description |
|---|---|---|
| $\alpha_1$ | $2.30 \times 10^{-1}$ day$^{-1}$ | Proliferative growth rate of $N$ |
| $\alpha_2$ | $6.72 \times 10^{-1}$ mm$^{-3}$ | Rate of influence of M2 on tumour volume |
| $\alpha_3$ | $7.00 \times 10^{-1}$ day$^{-1}$ | Growth rate of $M_1$ |
| $\alpha_4$ | $7.00 \times 10^{-1}$ (mm$^3$·day)$^{-1}$ | Rate of influence of $N$ on the proliferation of $M_2$ |
| $\alpha_5$ | $8.00 \times 10^{-1}$ (mm$^3$·day)$^{-1}$ | Rate of influence of $M_1$ on the proliferation of CD8+ |
| $\rho_1$ | $1.00 \times 10^{-2}$ (mm$^3$·day)$^{-1}$ | Polarisation rate from $M_1$ to $M_2$ |
| $\rho_2$ | $[0;\ 0.2]$ (mm$^3$·day)$^{-1}$ | Polarisation rate from $M_2$ to $M_1$ |
| $\beta_1$ | 1.344 (mm$^3$·day)$^{-1}$ | Rate of effectiveness of $M_1$ in fighting $N$ cells |
| $\beta_2$ | 4.312 (mm$^3$·day)$^{-1}$ | Rate of effectiveness of CD8+ in fighting $N$ cells |
| $\beta_3$ | 1.344 (mm$^3$·day)$^{-1}$ | Rate of effectiveness of $M_2$ in fighting CD8+ cells |
| $\mu_1$ | 0.87 day$^{-1}$ | Death rate of $M_1$ cells |
| $\mu_2$ | $1.00 \times 10^{-1}$ day$^{-1}$ | Death rate of $M_2$ cells |
| $\mu_3$ | $4.00 \times 10^{-1}$ day$^{-1}$ | Death rate of CD8+ cells |
| $K_n$ | 1 mm$^{-3}$ | Carrying capacity of neoplastic cells |
| $K_m$ | 1 mm$^{-3}$ | Carrying capacity of macrophages |
| $K_t$ | 1 mm$^{-3}$ | Carrying capacity of CD8+ cells |
| $\lambda$ | $10^{-2}$ day$^{-1}$ | Differentiation rate |
| $m_0$ | 1 mm$^{-3}$ | Cytokine concentrations in the tumour microenvironment |
| $\Phi$ | $[0;\ 400]$ mg(m$^2$·day)$^{-1}$ | Amount of chemotherapy |
| $\theta$ | 0.3 day$^{-1}$ | Absorption rate |
| $a_1$ | $10^{-2}$ m$^2$(mg day)$^{-1}$ | Predation coefficient on $N$ cells |
| $a_2$ | $4.0 \times 10^{-2}$ m$^2$(mg day)$^{-1}$ | Predation coefficient on $M_1$ cells |
| $a_3$ | $4.0 \times 10^{-2}$ m$^2$(mg day)$^{-1}$ | Predation coefficient on $M_2$ cells |
| $a_4$ | $3.0 \times 10^{-2}$ m$^2$(mg day)$^{-1}$ | Predation coefficient on $T_8$ cells |
| $b_i$ | 1 | Support rate when there is no competition and predation |

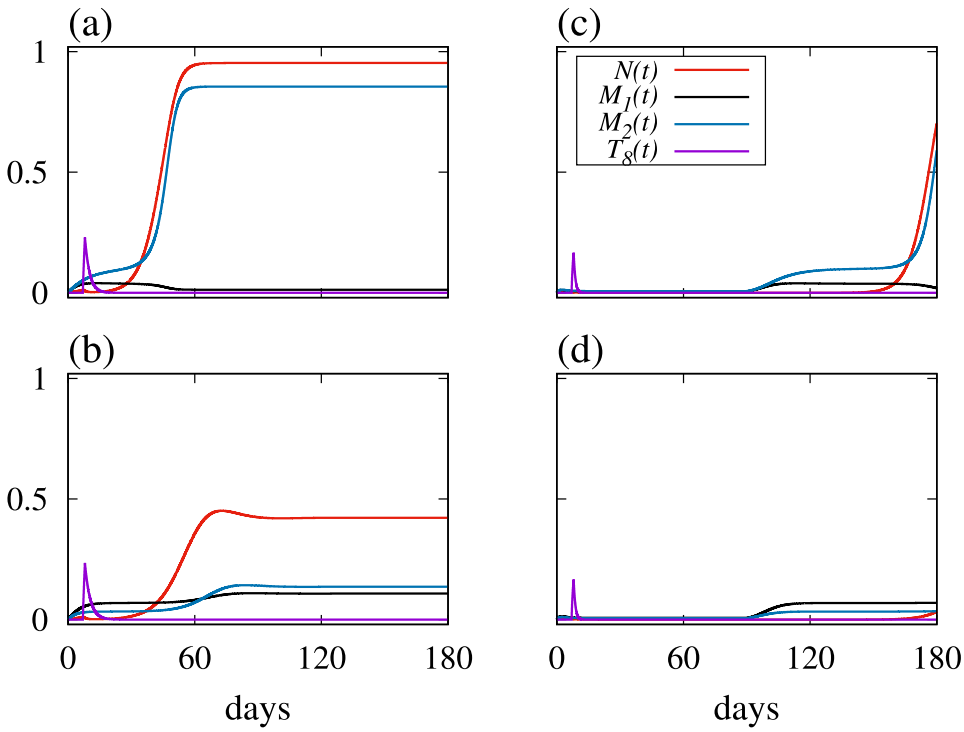


**Fig. 2** Temporal evolution of $N$ (red line), $M_1$ (black line), $M_2$ (cyan line), and $T_8$ (magenta line) for parameter values according to Table 1. The panels (**a**) and (**b**) display the solutions without chemotherapy ($\Phi = 0$) for $\rho_2 = 0$ and $\rho_2 = 0.2$, respectively. With chemotherapy ($\Phi = 10$), the panels (**c**) and (**d**) exhibit the solutions for $\rho_2 = 0$ and $\rho_2 = 0.2$

$T_8$ (magenta line) for parameter values listed in Table 1. Without chemotherapy ($\Phi = 0$) and no repolarisation stimulus ($\rho_2 = 0$), $N$ and $M_2$ increase while $M_1$ and $T_8$ go to zero, as shown in Fig. 2(a). Considering the macrophage repolarisation ($\rho_2 = 0.2$), the neoplastic cells value $N$ stabilises before reaching its maximum value due to the recruitment of macrophages from $M_2$ to $M_1$, as displayed in Fig. 2(b). Figures 2(c) and 2(d) exhibit the population dynamics of the cells with the administration of chemotherapeutic agents ($\Phi = 10$). Comparatively, Fig. 2(d) displays a lower $N$ value in 180 days compared to that exhibited in Fig. 2(c). It is due to the combination of chemotherapy with immunotherapy, known as chemoimmunotherapy. A pronounced peak in the $T_8$ population occurs due to the TIL injection at $t = 7$, followed by clonal expansion and subsequent cell death or exhaustion.

## 3 Pulsed Chemotherapy

In pulsed chemotherapy, the drugs are administered in cycles with periods of rest. The repeated application of drugs for a short time presents some benefits including reduced side effects and delayed drug resistance. There are different clinical protocols associated with the pulsed chemotherapy.

Figure 3 displays the population dynamics of the cells for $\rho_2 = 0.2$ and $m_0 = 1$. In our simulations, we consider the protocols (a) $1\times7$ with $\Phi = 200$ for 15 cycles, (b) $1\times14$ with $\Phi = 200$ for 8 cycles, (c) $1\times21$ with $\Phi = 200$ for 6 cycles, and (d) $1\times7$ plus $1\times28$ with $\Phi_1 = 50$ and $\Phi_2 = 150$, respectively, for 15 cycles and 4 cycles each one. The red line corresponds to the neoplastic cells $N(t)$, the black line represents the macrophages of type $M_1(t)$, the cyan line denotes the macrophages of type $M_2(t)$, and the magenta line represents the immune system cells $T_8(t)$. The number of neoplastic cells grows and reaches an asymptotic state. We observe that the time for $N$ to reach an asymptotic state depends on the protocol.

We analyse the post-treatment status by means of the time ($\tau$) that the tumour takes to regrow after stopping the chemotherapy. Figure 4 shows the parameter space $\rho_2 \times \Phi$ for different protocols. The colour bar exhibits the $\tau$ values that are obtained after the end of the treatment cycles according to the protocols. The panels (a), (b), (c), and (d) correspond to the protocols $1\times7$, $1\times14$, $1\times21$, and $1\times7$ plus $1\times28$, respectively. The red region represents a longer life expectancy and the blue region denotes a shorter one. The size of the red region is larger for the protocols $1\times7$ (Fig. 4(a)) and $1\times7$ plus $1\times28$ (Fig. 4(d)). The protocol $1\times14$ has a red region larger than the protocol $1\times21$, as shown in Fig. 4(b) and Fig. 4(c). Increasing the rest days, we verify that large $\tau$ values are observed for larger $\Phi$ values. Comparing the panels (a), (b), and (c), a shorter interval between chemotherapy treatments is better to increase the survival time. Figure 4(d) shows that combined chemotherapy protocols can also be used to enhance the survival time after the end of the cycles (red region), where $\Phi = \Phi_1 \in [0, 400]$ and $\Phi_2 = 3 \times \Phi_1$.

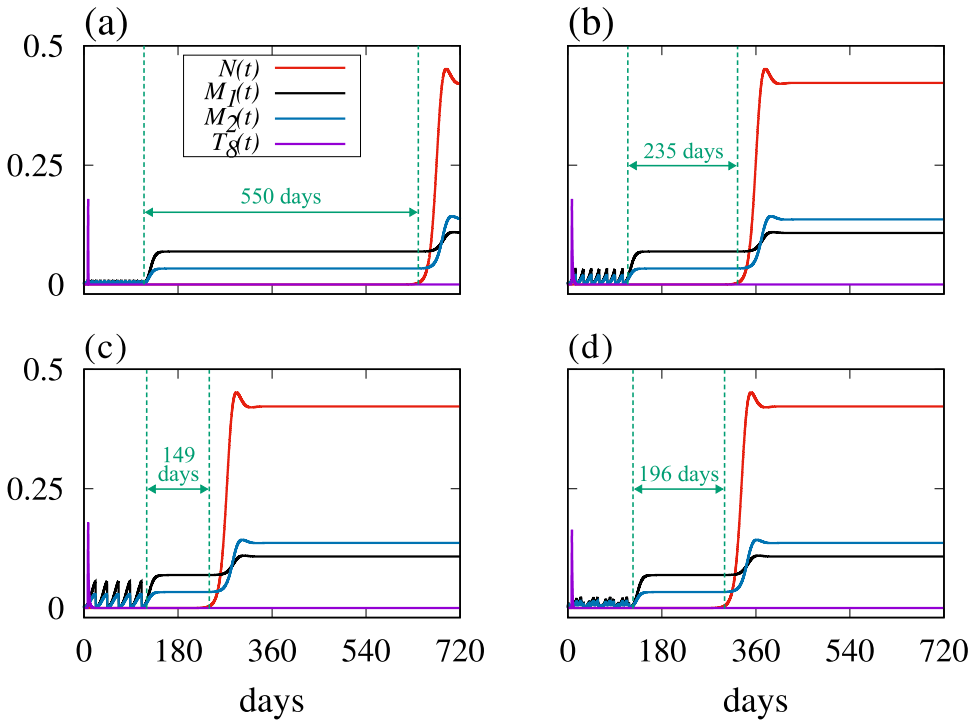


**Fig. 3** Temporal evolution of $N$ (red line), $M_1$ (black line), $M_2$ (cyan line), and $T_8$ (magenta line) for $\rho_2 = 0.2$ and $m_0 = 1$. (**a**) $1 \times 7$ with $\Phi = 200$ for 15 cycles ($\tau = 500$ days), (**b**) $1 \times 14$ with $\Phi = 200$ for 8 cycles ($\tau = 235$ days), (**c**) $1 \times 21$ with $\Phi = 200$ for 6 cycles ($\tau = 149$ days), and (**d**) $1 \times 7$ plus $1 \times 28$ with $\Phi_1 = 50$ and $\Phi_2 = 150$ ($\tau = 196$ days), respectively, for 15 cycles and 4 cycles each one

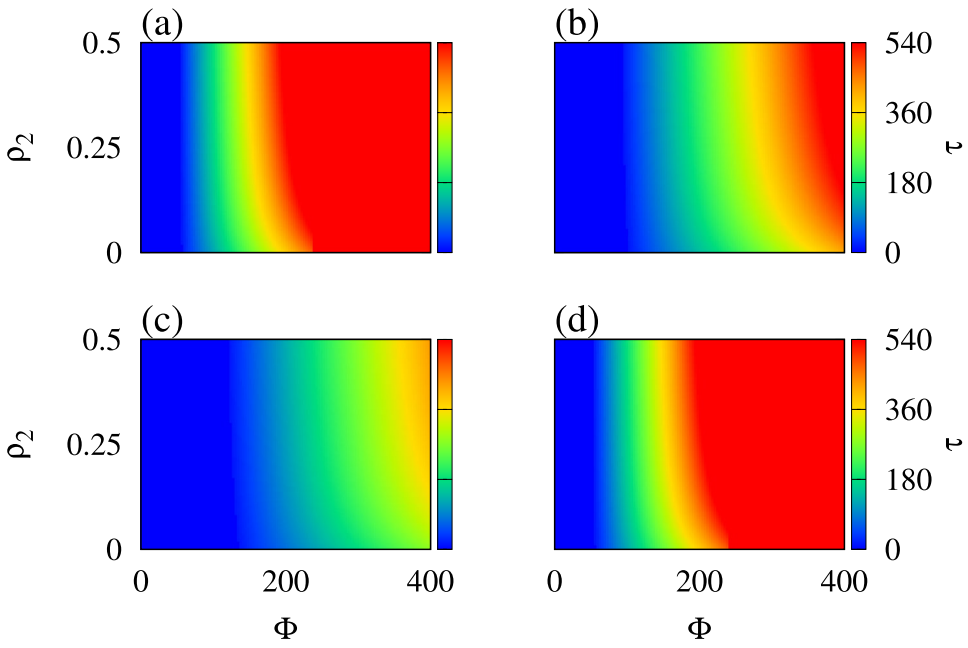


**Fig. 4** Parameter space $\rho_2 \times \Phi$ for (**a**) $1 \times 7$ with 15 cycles, (**b**) $1 \times 14$ with 8 cycles, (**c**) $1 \times 21$ with 6 cycles, and (**d**) $1 \times 7$ plus $1 \times 28$ ($\Phi = \Phi_1 \in [0, 400]$ and $\Phi_2 = 3 \times \Phi_1$) with 16 and 5 cycles, respectively. We consider $v(t) = 0.2857$ ($t \in [7, 8]$) and $v(t) = 0$ ($t \in (-\infty, 7) \cup (8, \infty)$). The colour bar represents the survival time ($\tau$) after the end of the cycles. The red region corresponds to a longer life expectancy and the blue region denotes a shorter one

**Table 2** Amount of chemotherapy per cycle, where $\Phi_{1,2}$=$\Phi_{1,2}$

| | $1 \times 7$ | $1 \times 14$ | $1 \times 21$ | $1 \times 7$+$1 \times 21$ |
|---|---|---|---|---|
| Brown | 83.13 | 147.78 | 221.67 | $\Phi_{1,2}$=30, 170 |
| Black | 90 | 160 | 240 | $\Phi_{1,2}$=40, 160 |
| Green | 96.88 | 172.22 | 258.33 | $\Phi_{1,2}$=50, 150 |
| Blue | 103.75 | 184.44 | 276.67 | $\Phi_{1,2}$=60, 140 |
| Red | 117.50 | 208.89 | 313.33 | $\Phi_{1,2}$=80, 120 |

The colours correspond to $\bar{\tau}$ in Fig. 5

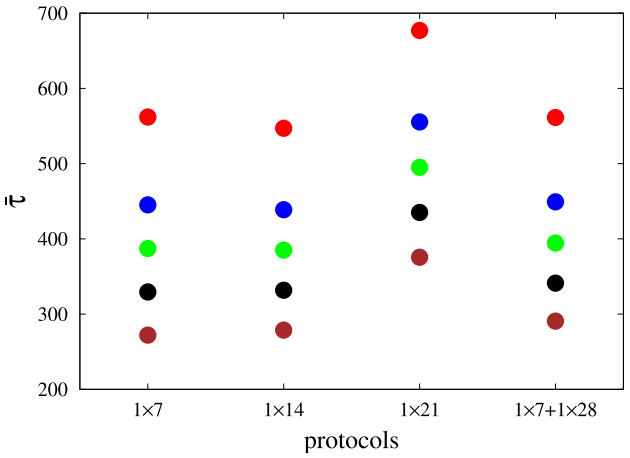


**Fig. 5** $\bar{\tau}$ for different protocols, $\rho_2 = 0.2$, $m_0 = 1$, and amount of chemotherapy according to Table 2. We consider 1000 different initial conditions to calculate $\bar{\tau}$

Considering that the total amount of drug administered until the final course of chemotherapy is approximately the same for all protocols, we compute the averaged $\tau$ values ($\bar{\tau}$) for 1000 different initial conditions. Table 2 shows the amount of chemotherapy ($\Phi$) per cycle in each protocol, where the colour names in the first column indicate the ones used in Fig. 5.

Figure 5 displays $\bar{\tau}$ for different protocols, $\rho_2 = 0.2$, $m_0 = 1$, and amount of chemotherapy according to Table 2. For the three protocols and combined protocols, we observe an increase in $\bar{\tau}$ when the amount of chemotherapy per cycle is increased ($\Phi$ and $\Phi_1$). For the protocols $1 \times 7$, $1 \times 14$, and $1 \times 7 + 1 \times 28$, the values of $\bar{\tau}$ are approximately equal. The protocol $1 \times 21$ show higher $\bar{\tau}$ values for all amount of chemotherapy per cycle.

The chemoimmunotherapy is a treatment that combines chemotherapy with immunotherapy. Chemotherapeutic agents are used to eliminate cancer cells and the immune system is stimulated or restored to fight cancer. To analyse the influence of the chemotherapy and immune system, we compute the parameter space $v(t) \times \Phi$ for (a) $1 \times 7$ with 15 cycles, (b) $1 \times 14$ with 8 cycles, (c) $1 \times 21$ with 6 cycles, and (d) $1 \times 7$ plus $1 \times 28$ ($\Phi = \Phi_1 \in [0, 400]$ and $\Phi_2 = 3 \times \Phi_1$) with 16 and 5 cycles, respectively, as displayed in Fig. 6. The colour bar correspond to the $\tau$ values. We consider $v(t)$ in the interval [0, 1] and the tumour-infiltrating lymphocytes

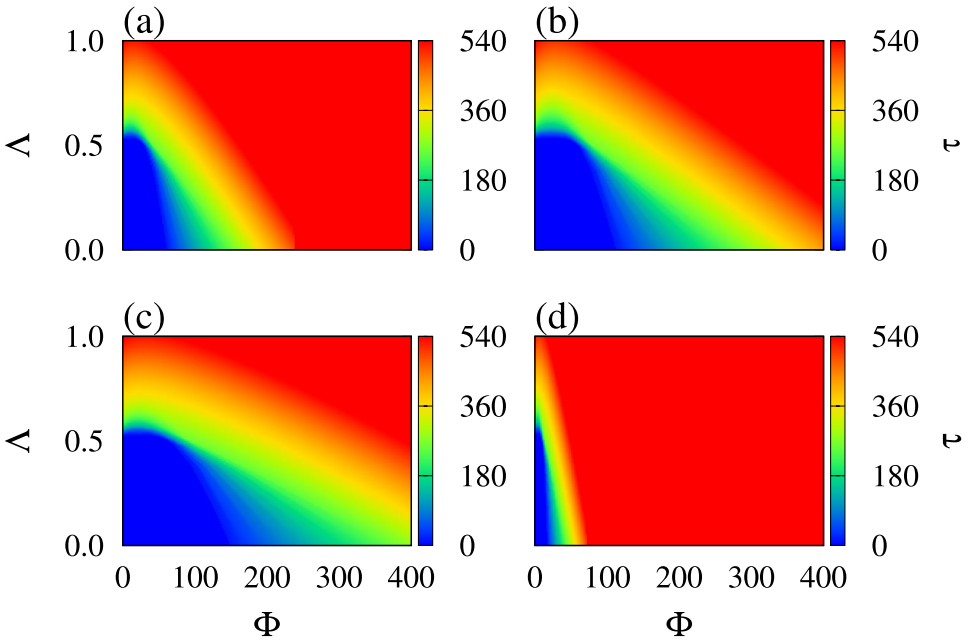


**Fig. 6** Parameter space $\Lambda \times \Phi$ for (**a**) $1 \times 7$ with 15 cycles, (**b**) $1 \times 14$ with 8 cycles, (**c**) $1 \times 21$ with 6 cycles, and (**d**) $1 \times 7$ plus $1 \times 28$ ($\Phi = \Phi_1 \in [0, 400]$ and $\Phi_2 = 3 \times \Phi_1$) with 16 and 5 cycles, respectively. We consider $v(t) = \Lambda$ ($t \in [7, 8]$) and $v(t) = 0$ ($t \in (-\infty, 7) \cup (8, \infty)$). The colour bar represents the survival time ($\tau$) after the end of the cycles

doses are applied continuously between 7th and 8th days with 29 days of cycle. Larger and smaller $\tau$ values are represented by red and blue, respectively. For all protocols, we observe that chemotherapy and immunotherapy can be more effective when combined.

## 4 Conclusions

Chemoimmunotherapy is a treatment option for cancer that combines chemotherapy and immunotherapy. The chemotherapeutic agents eliminate or slow down the growth of cancerous cells. The immunotherapy improves the immune system to recognise and attack the cancer. In this work, we study the non-small cell lung cancer (NSCLC) control based on chemoimmunotherapy. The NSCLC is the most common type of lung cancer.

We include chemotherapy in a NSCLC model with immunotherapy. Due to the immunotherapy, there are processes of repolarisation of macrophages within the microenvironment combined with the infiltration of lymphocytes into the tumour. Considering three months of chemotherapy, it is possible to observe a reduction in the number of cancer cells.

We analyse the post-treatment status by means of the time ($\tau$) that the tumour takes to regrow after stopping the pulsed chemotherapy. To do that, we consider the protocols $1 \times 7$ with 15 cycles, $1 \times 14$ with 8 cycles, $1 \times 21$ with 6 cycles, and $1 \times 28$ plus $1 \times 28$ with 16 and 5 cycles. By varying the polarisation rate of the number of macrophage phenotype from 2 to 1 and the amount of chemotherapy, the protocols $1 \times 7$ and $1 \times 7$ plus $1 \times 28$ exhibit better parameter ranges for the $\tau$ values. For all protocols, maintaining approximately the same total amount of drug administered until the final course of chemotherapy, the protocol $1 \times 21$ show the best results for the averaged $\tau$ values.

Recently, Hirabayashi et al. [34] examined real-world data after the introduction of chemoimmunotherapy in patients with cell lung cancer. They reported that the median overall survival in chemotherapy and chemoimmunotherapy were 9.7 and 15 months, respectively. Depending on the treatment protocol, our results show a range of survival time approximately between 10 and 20 months, a median overall survival equal to 15 months.

With regard to chemoimmunotherapy in NSCLC control, we show that the treatment can prolong the patient survival in the context of protocols. The combination of chemotherapeutic agents with immune therapy plays an important role in the cancer treatment effectiveness.

**Acknowledgements** This work was possible by partial financial support from the following Brazilian government agencies: CNPq, CAPES, Fundação Araucária and FAPESP (2024/05700-5, 2025/02318-5). E.C.G. received partial financial support from Coordenação de Aperfeiçoamento de Pessoal de Nível Superior - Brasil (CAPES) - Finance Code 88881.846051/2023-01. We would like to thank www.105groupscience.com.

**Author Contributions** Ana P.S. Koltun, Moises S. Santos, José Trobia, Fernando S. Borges, Kelly C. Iarosz, Iberê L. Caldas, Enrique C. Gabrick, Diogo L. M. Souza, Fátima E. Cruziniani and Antonio M. Batista contributed equally to this work.

**Data Availability** No datasets were generated or analysed during the current study.

## Declarations

**Conflicts of Interest** The authors declare no conflict of interest. None of the authors hold any editorial role within the journal, ensuring an unbiased and independent research process.

**Competing interests** The authors declare no competing interests.

## References


1. D.M. Hausman, What is cancer? Perspect. Biol. Med. **62**, 778–784 (2019)
2. R.L. Siegel, A.N. Giaquinto, A. Jemal, Cancer statistics, 2024. CA Cancer J. Clin. **74**, 12–49 (2024)
3. W.D. Travis, Pathology of lung cancer. Clin. Chest Med. **32**, 669–692 (2011)
4. R. Sulimanov, K. Koshelev, V. Makarov, A. Mezentsev, M. Durymanov, L. Ismail, K. Zahid, Y. Rumyantsev, I. Laskov, Mathematical modeling of non-small-cell lung cancer biology through the experimental data on cell composition and growth of patient-derived organoids. Life **13**, 2228 (2023)
5. E. Lourenço, D.S. Rodrigues, M.E. Antunes, P.F.A. Mancera, G. Rodrigues, A simple mathematical model of non-small cell lung cancer involving macrophages and CD8+ T cells. J. Biol. Syst. **31**, 1407–1431 (2023)
6. B. Stankovic, H.A.K. Bjorhovde, R. Skarshaug, H. Aamodt, A. Frafjord, E. Müller, C. Hammarström, K. Beraki, E.S. Baekkevold, P.R. Woldbaek, A. Helland, O.T. Brustugun, I. Oynebraten, A. Corthay, Immune cell composition in human non-small cell lung cancer. Front. Immunol. **9**, 3101 (2019)
7. M. Qomlaqi, F. Bahrami, M. Ajami, J. Hajati, An extended mathematical model of tumor growth and its interaction with the immune system, to be used for developing an optimized immunotherapy treatment protocol. Math. Biosci. **292**, 1–9 (2017)
8. J.A. McKnight, Principles of chemotherapy. Clin. Tech. Small Anim. Pract. **18**, 67–72 (2003)
9. Z. Zhang, S. Li, P. Si, X. Li, X. He, A tumor-immune model with mixed immunotherapy and chemotherapy: qualitative analysis and optimal control. J. Biol. Syst. **30**, 339–364 (2022)
10. C. Letellier, S.K. Sasmal, C. Draghi, F. Denis, D. Ghosh, A chemotherapy combined with an anti-angiogenic drug applied to a cancer model including angiogenesis. Chaos Soliton Fract. **99**, 297–311 (2017)
11. W. Liu, T. Hillen, H.I. Freedman, A mathematical model for M-phase specific chemotherapy including the $G_0$ -phase and immunoresponse. Math. Biosci. Eng. **4**, 239–259 (2007)
12. F.S. Borges, K.C. Iarosz, H.P. Ren, A.M. Batista, M.S. Baptista, R.L. Viana, S.R. Lopes, C. Grebogi, Model for tumour growth with treatment by continuous and pulsed chemotherapy. Biosyst. **116**, 43–48 (2014)
13. J.Y. Douillard, R. Rosell, M. De Lena, F. Carpagnano, R. Ramlau, J.L. Gonzáles-Larriba, T. Grodzki, J.R. Pereira, A. Le Groumellec, V. Lorusso, C. Clary, Adjuvant vinorelbine plus cisplatin versus observation in patients with completely resected stage IB-IIIA non-small-cell lung cancer (Adjuvant Navelbine International Trialist Association [ANITA]): a randomised controlled trial. Lancet Oncol. **7**, 719–727 (2006)
14. J.Y. Douillard, R. Rosell, M. De Lena, M. Riggi, P. Hurteloup, M.A. Mahe, Adjuvant Navelbine International Trialist Association, Impact of postoperative radiation therapy on survival in patients with complete resection and stage I, II, or IIIA non–small-cell lung cancer treated with adjuvant chemotherapy: the adjuvant Navelbine International Trialist Association (ANITA) randomized trial. Int. J. Radiat. Oncol. Biol. Phys. **72**, 695–701 (2008)
15. J.H. Schiller, D. Harrington, C.P. Belani, C. Langer, A. Sandler, J. Krook, J. Zhu, D.H. Johnson, Comparison of four chemotherapy regimens for advanced non-small-cell lung cancer. N. Engl. J. Med. **346**, 92–98 (2002)
16. F.V. Fossella, Second-line chemotherapy for non-small-cell lung cancer. Curr. Oncol. Rep. **2**, 96–101 (2000)
17. A. Inoue, N. Saijo, Recent advances in the chemotherapy of non-small cell lung cancer. Jpn. J. Clin. Oncol. **31**, 299–304 (2001)
18. R.N. Younes, J.R. Pereira, A.L. Fares, J.L. Gross, Chemotherapy beyond first-line in stage IV metastatic non-small cell lung cancer. Rev. Assoc. Med. Bras. **57**, 686–691 (2011)
19. A. Chang, Chemotherapy, chemoresistance and the changing treatment landscape for NSCLC. Lung Cancer **71**, 3–10 (2011)
20. S.E. Rebuzzi, R. Alfieri, S. La Monica, R. Minari, P.G. Petronini, M. Tiseo, Combination of EGFR-TKIs and chemotherapy in advanced EGFR mutated NSCLC: review of the literature and future perspectives. Crit. Rev. Oncol. Hematol. **146**, 102820 (2020)
21. J. Kaur, J. Elms, A.L. Munn, D. Good, M.Q. Wei, Immunotherapy for non-small cell lung cancer (NSCLC), as a stand-alone and in combination therapy. Crit. Rev. Oncol. Hematol. **164**, 103417 (2021)
22. A.D. Waldman, J.M. Fritz, M.J. Lenardo, A guide to cancer immunotherapy: from T cell basic science to clinical practice. Nat. Rev. Immunol. **20**, 651–668 (2020)
23. E. Brambilla, G. Le Teuff, S. Marguet, S. Lantuejoul, A. Dunant, S. Graziano, R. Pirker, J.Y. Douillard, T. Le Chevalier, M. Filipits, R. Rosell, R. Kratzke, H. Popper, J.C. Soria, F.A. Shepherd, L. Seymour, M.S. Tsao, Prognostic effect of tumor lymphocytic infiltration in resectable non–small-cell lung cancer. J. Clin. Oncol. **34**, 1223–1230 (2016)
24. A.P.S. Koltun, J. Trobia, A.M. Batista, E.K. Lenzi, M.S. Santos, F.S. Borges, K.C. Iarosz, I.L. Caldas, E.C. Gabrick, Fractional tumour-immune model with drug resistance. Braz. J. Phys. **54**, 41 (2024)
25. J. Trobia, K. Tian, A.M. Batista, C. Grebogi, H.P. Ren, M.S. Santos, P.R. Protachevicz, F.S. Borges, J.D. Szezech Jr., R.L. Viana, I.L. Caldas, K.C. Iarosz, Mathematical model of brain tumour growth with drug resistance. Commun. Nonlinear Sci. Numer. Simul. **103**, 106013 (2021)
26. J. Trobia, E.C. Gabrick, E.G. Seifert, F.S. Borges, P.R. Protachevicz, J.D. Szezech Jr., K.C. Iarosz, M.S. Santos, I.L. Caldas, K. Tian, H.P. Ren, C. Grebogi, A.M. Batista, Effects of drug resistance in the tumour-immune system with chemotherapy treatment. Indian Acad. Sci. Conf. Ser. **3**, 1–6 (2020)
27. K.C. Iarosz, F.S. Borges, A.M. Batista, M.S. Baptista, R.A.N. Siqueira, R.L. Viana, S.R. Lopes, Mathematical model of brain tumour with glia–neuron interactions and chemotherapy treatment. J. Theor. Biol. **368**, 113–121 (2015)
28. G.E. Mahlbacher, K.C. Reihmer, H.B. Frieboes, Mathematical modeling of tumor-immune cell interactions. J. Theor. Biol. **469**, 47–60 (2019)
29. A.R. Anderson, V. Quaranta, Integrative mathematical oncology. Nat. Rev. Cancer **8**, 227–234 (2008)
30. S. Das, G. Mandal, S. Dutta, L.N. Guin, K. Chakravarty, Analysis and regulation of chaos dynamics in a cancer model through chemotherapeutic intervention and immune system augmentation. Int. J. Dynam. Control **12**, 3884–3907 (2024)
31. R. Eftimie, C. Barelle, Mathematical investigation of innate immune responses to lung cancer: the role of macrophages with mixed phenotypes. J. Theor. Biol. **524**, 110739 (2021)
32. I. Diaz-Cano, L. Paz-Ares, I. Otano, Adoptive tumor infiltrating lymphocyte transfer as personalized immunotherapy. in

*International Review of Cell and Molecular Biology*, (Academic Press 2022), **370**, 163–192
33. M. Reis-Sobreiro, A.T. Da Mota, C. Jardim, K. Serre, Bringing macrophages to the frontline against cancer: current immunotherapies targeting macrophages. Cells **10**, 2364 (2021)
34. T. Hirabayashi, K. Sonehara, T. Tsutsui, S. Nozawa, T. Agatsuma, M. Yamamoto, A. Matsuo, M. Nakanishi, T. Chiaki, A. Kato, T. Miyahara, T. Hachiya, S. Kanda, K. Yanagisawa, T. Araki, K. Tateishi, M. Hanaoka, Real-world data after introduction of chemoimmunotherapy in patients with extensive-disease small cell lung cancer: a multicenter retrospective study. Respir. Investig. **63**, 928–933 (2025)